

# Trends of neutron skins and radii of mirror nuclei from first principles

S. J. Novario,<sup>1</sup> D. Lonardoni,<sup>1</sup> S. Gandolfi,<sup>1</sup> and G. Hagen<sup>2,3</sup>

<sup>1</sup>*Theoretical Division, Los Alamos National Laboratory, Los Alamos, NM 87545, USA*

<sup>2</sup>*Physics Division, Oak Ridge National Laboratory, Oak Ridge, TN 37831, USA*

<sup>3</sup>*Department of Physics and Astronomy, University of Tennessee, Knoxville, TN 37996, USA*

The neutron skin of atomic nuclei impacts the structure of neutron-rich nuclei, the equation of state of nucleonic matter, and the size of neutron stars. Here we predict the neutron skin of selected light and medium-mass nuclei using coupled-cluster theory and the auxiliary field diffusion Monte Carlo method with two- and three-nucleon forces from chiral effective field theory. We find a linear correlation between the neutron skin and the isospin asymmetry and compare with data. We also find a linear relationship between proton and neutron radii of mirror nuclei and quantify the effect of charge symmetry breaking. Our results for the mirror-difference charge radii and binding energies per nucleon agree with existing data.

*Introduction.*— The size of neutron stars and the distributions of excess neutrons in medium-mass and heavy nuclei can be linked to the microscopic forces between the constituent nucleons that build up the atomic nucleus and the equation-of-state (EoS) of nucleonic matter [1–4]. With recent advancements in both observational astrophysics and experimental nuclear physics, investigating this link and constraining nuclear models is now becoming possible. The advent of multimessenger astronomy, established with the simultaneous observation of a binary neutron star merger by the LIGO gravitational-wave observatory [5, 6] and gamma-ray astronomy, has opened up the possibility of examining the structure of neutron stars in new detail [7]. Furthermore, state-of-the-art experiments designed to precisely measure the neutron distributions in nuclei, including the recent neutron skin measurement of  $^{208}\text{Pb}$  by PREX [8, 9] and  $^{48}\text{Ca}$  by CREX [10, 11], are now being confronted by theory.

The neutron skin thickness,  $\Delta R_{\text{np}}$ , is defined as the difference between the root-mean-squared (rms) point radii of the neutron and proton density distributions. Collectively, the neutron skin results from a balance between the inward pressure of the surface tension on excess neutrons on the edge of the nucleus and outward degeneracy pressure from excess neutrons within the core of the nucleus. The same balance is reached in neutron stars with the inward pressure of gravity. The relationship between this pressure and the neutron density is quantified in the slope of the symmetry energy at saturation density,  $L$ . Therefore, this bulk property of neutron stars should be related to the neutron skin of nuclei [1, 2, 12–16].

Recent high-precision measurements of charge radii in isotope chains of potassium [17], calcium [18, 19], nickel [20], copper [21, 22], and silver [23], have revealed that they carry information about changes in shell-structure, deformation, and pairing effects. Charge radii can be easily probed with the well-known electromagnetic interaction [24, 25]. Conversely, measuring the neutron (weak-charge) radius is more difficult, but can be accomplished using either strong or electroweak probes, each with their own shortcomings. Hadronic probes suffer from model-

dependent uncertainties [26], and electroweak probes, like those used in PREX [8, 9] and CREX [10, 11], are less model-dependent but are hindered by one-part-per-million parity-violating asymmetry [27]. This hurdle can be overcome in some cases [8, 9], but precision measurements of the neutron radius for short-lived isotopes remain elusive.

In this Letter, we study trends in the neutron skin thickness of light and medium-mass mirror nuclei with mass number  $6 \leq A \leq 56$  (shown in Fig. 1) by computing the proton and neutron radii using the *ab initio* coupled-cluster (CC) [28–34] and auxiliary field diffusion Monte Carlo (AFDMC) methods [35–37], each with different nuclear interactions derived from chiral effective field theory

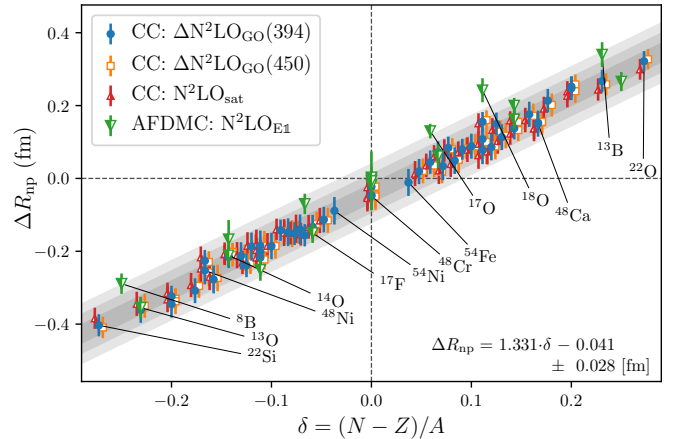


Figure 1. Neutron skin thickness plotted against the isospin asymmetry from *ab initio* calculations. Coupled-cluster results of nuclei with  $14 \leq A \leq 56$  using the  $\Delta\text{N}^2\text{LO}_{\text{G}0}(394)$ ,  $\Delta\text{N}^2\text{LO}_{\text{G}0}(450)$ , and  $\text{N}^2\text{LO}_{\text{sat}}(450)$  interactions are shown as solid blue circles, empty orange squares, and right-filled red triangles, respectively. Left-filled green triangles represent auxiliary field diffusion Monte Carlo results for  $6 \leq A \leq 18$  using the  $\text{N}^2\text{LO}_{\text{E}1}$  local chiral interaction. The linear regression is printed in the bottom right with  $1\sigma$  uncertainty, and the  $1\sigma$ ,  $2\sigma$ , and  $3\sigma$  confidence levels are shown as overlapping gray bands. Select nuclei are labeled.

(described below). We then establish a simple and robust relation between these data and the isospin asymmetry of the various nuclei and use this relation to estimate the neutron skin of relevant heavy nuclei not directly calculated in this work. Additionally, we use the isospin symmetry of mirror nuclei to develop a relation between the proton and neutron radii of mirror partners and compare our computed mirror-difference charge radii and binding energies per nucleon with available data. Finally, we estimate the contribution of the isospin-symmetry-breaking terms by turning off the Coulomb interaction.

*Methods.*— We describe nuclei as a collection of  $A$  point-like nucleons of mass  $m$  interacting according to the non-relativistic intrinsic Hamiltonian

$$H = -\frac{\hbar^2}{2mA} \sum_{i<j} (\nabla_i - \nabla_j)^2 + \sum_{i<j} V_{ij} + \sum_{i<j<k} V_{ijk}. \quad (1)$$

Here,  $V_{ij}$  and  $V_{ijk}$  are the nucleon-nucleon (NN) and three-nucleon (NNN) potentials, respectively, the former of which also includes the Coulomb force. Interactions used in this work are derived from chiral effective field theory (EFT) [38–45]. The CC calculations use three different chiral interactions. The first,  $N^2\text{LO}_{\text{sat}}$  [46], was optimized to few-body observables as well as radii and ground-state energies of selected carbon and oxygen isotopes. The second and third,  $\Delta N^2\text{LO}_{\text{GO}}(394)$  and  $\Delta N^2\text{LO}_{\text{GO}}(450)$  [47–49], include explicit  $\Delta$ -isobars and were optimized to few-body observables and properties of nucleonic matter, and use momentum cutoff of  $\Lambda = 394$  MeV/c and  $\Lambda = 450$  MeV/c, respectively.

After establishing the nuclear interactions, we perform a Hartree-Fock diagonalization from a spherical harmonic-oscillator basis and then construct a prolate, axially-deformed product state built from natural orbitals [50, 51]. We then normal-order the Hamiltonian with respect to the reference state, denoted by  $|\Phi_0\rangle$ , and retain one- and two-body terms [52, 53]. Next, we use the coupled-cluster method in the singles-and-doubles (CCSD) approximation to construct the similarity-transformed Hamiltonian,  $\bar{H}_N = e^{-\hat{T}} H_N e^{\hat{T}}$ , which decouples the reference state from excitations around it. In the CCSD approximation the cluster operator,  $\hat{T}$ , is truncated at the  $2p$ - $2h$  excitation level. Because  $\hat{T}$  is asymmetric,  $\bar{H}_N$  is non-Hermitian, and the left ground state must be decoupled separately using  $\langle \Phi_0 | (1 + \hat{\Lambda})$ , where  $\hat{\Lambda}$  is a de-excitation analogue to  $\hat{T}$  [33, 34] and is also truncated at the  $2p$ - $2h$  level. In this work we are interested in computing the ground-state expectation value of the squared intrinsic point-nucleon radius operator,  $\hat{r}^2$ . In CC theory this operator is similarity transformed according to,  $\bar{r}^2 \equiv e^{-\hat{T}} \hat{r}^2 e^{\hat{T}}$ , and applied between the left and right CC ground states, *i.e.*,  $\langle \hat{r}^2 \rangle \equiv \langle \Phi_0 | (1 + \hat{\Lambda}) \bar{r}^2 | \Phi_0 \rangle$ .

We also perform AFDMC calculations of the point-proton and neutron radii (see Ref. [37] for more details)

using a local chiral nucleon-nucleon and three-nucleon interaction at next-to-next-to-leading order,  $N^2\text{LO}_{\text{E1}}$  [37, 54–56]. This interaction has been used to study the ground-state properties of nuclei up to  $^{16}\text{O}$  [37, 56–64], few neutron systems [65–67], and neutron star matter [55, 56, 68–77].

*Results.*— Our results for the neutron skin thickness of selected nuclei with  $6 \leq A \leq 56$  are shown in Fig. 1. These data are plotted against the isospin asymmetry,  $\delta = (N - Z)/A$ , with  $N$  and  $Z$  being the number of neutrons and protons, respectively. As can be seen, there is a linear relation between the neutron skin thickness and the isospin asymmetry which is robust across different *ab initio* methods and chiral interactions. This correlation was first derived in Ref. [78] from the liquid-drop model and demonstrated with mean-field methods. We fit the data using linear regression which is shown in Fig. 1 as shaded gray bands at  $1\sigma$ ,  $2\sigma$ , and  $3\sigma$  confidence levels.

There are several distinct sources of uncertainties in the CC calculations. First, the error associated with the finite size of the employed model space is estimated by taking the difference between the point-nucleon radius calculated in the model spaces of  $N_{\text{max}} = 12$  and  $N_{\text{max}} = 10$ , respectively, where  $N_{\text{max}} = (2n + l)_{\text{max}}$  indicates the maximum harmonic oscillator energy level. We also note that in this work we utilize a basis with an oscillator energy of  $\hbar\omega = 16$  MeV, which might not be optimal for all calculated nuclei. The additional uncertainty associated with this choice is estimated to be 1% [51, 79]. Second, the uncertainty associated with truncating the CC excitation operator at the  $2p$ - $2h$  level amounts to another 1% [51, 79, 80]. Finally, the error from breaking rotational symmetry is estimated to be less than 1% on computed radii (see Ref. [81] for details). Uncertainties on AFDMC results are statistical, and are reported in this work at the  $1\sigma$  confidence level. Errors on radii also include an extrapolation uncertainty from mix estimates, and those on binding energies from unconstrained evolution (see Ref. [37] for more details).

To test the validity of our linear relationship between neutron skin thickness and the isospin asymmetry, we plot the linear regression of our results at  $3\sigma$  confidence level with experimental data of neutron-rich nuclei in Fig. 2. Most of this data is extracted from  $X$ -ray spectroscopy following antiprotonic annihilation [82]. These data are used to fit a linear relationship which is shown as a green band [83]. Also shown are the results from PREX-I [8] and PREX-II [9], which measure the neutron radius of  $^{208}\text{Pb}$  using parity-violating electron scattering.

While our linear fit has a slightly larger slope than the antiprotonic X-ray data [83], our results overlap significantly with the experimental data and—using  $^{208}\text{Pb}$  as an indicator—lie in between the hadronic and electroweak data. Using our extracted linear relationship to predict the neutron-skin of  $^{208}\text{Pb}$  with  $\delta = 44/208$  we obtain  $\Delta R_{\text{np}}(^{208}\text{Pb}) = 0.241 \pm 0.028$  fm, consistent with

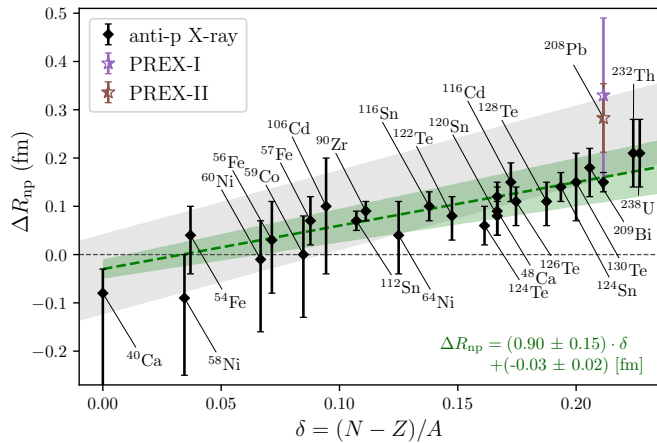


Figure 2. Neutron skin thickness plotted against the isospin asymmetry from available experimental data. Solid black diamonds are the results extracted from antiprotonic  $X$ -ray data [82, 83]. The right-filled purple star and the left-filled brown star are the values for  $^{208}\text{Pb}$  from PREX-I [8] and PREX-II [9], respectively. The green dashed line with band is the empirical evaluation of the relation, printed in the bottom right, from Ref. [83]. These experimental data are compared with the theoretical relation derived in Fig. 1, which is shown by the gray band.

the PREX-II result,  $\Delta R_{\text{np}}(^{208}\text{Pb}) = 0.283 \pm 0.071$  fm [9].

While this comparison relies on a precarious extrapolation from medium-mass to heavy nuclei, it could indicate the possibility of both a relatively large neutron skin in  $^{208}\text{Pb}$  with an interaction that corresponds to a realistic EoS of nucleonic matter. Specifically, the interactions used in this work give symmetry energy slopes at saturation of  $L = 58.4, 65.2$  MeV for the  $\Delta\text{N}^2\text{LO}_{\text{GO}}$  interactions [49],  $L = 40.8$  MeV for  $\text{N}^2\text{LO}_{\text{sat}}$  [13], and  $L = 59(9)$  MeV for  $\text{N}^2\text{LO}_{\text{E1}}$  [76]. This is in contrast to results from energy density functional theory that suggest that the relatively large neutron skin measurement from PREX-II corresponds to an unrealistic symmetry energy slope of  $L = 107 \pm 37$  MeV [84].

In addition to establishing a general equation for the neutron skin, we can also use our results to establish a relationship between the point-proton radius of a nucleus,  $R_{\text{p}}$  and the point-neutron radius of its mirror partner,  $R_{\text{n}}^{\text{mirror}}$ . In the limit of conserved isospin symmetry, these two quantities should be exactly equal. We show the resulting linear relationship in Fig. 3, the slope of which is just less than unity. This highlights the deviation from isospin symmetry, mostly due to the Coulomb interaction pushing the protons out to an extended distribution. The residuals between the data and the predictions from the linear model are also shown in Fig. 3, plotted against the isospin asymmetry. This linear relationship again highlights the underlying dependence on the isospin asymmetry for the neutron skin thickness. Combining the two linear fits in Fig. 3 results in the overall linear model con-

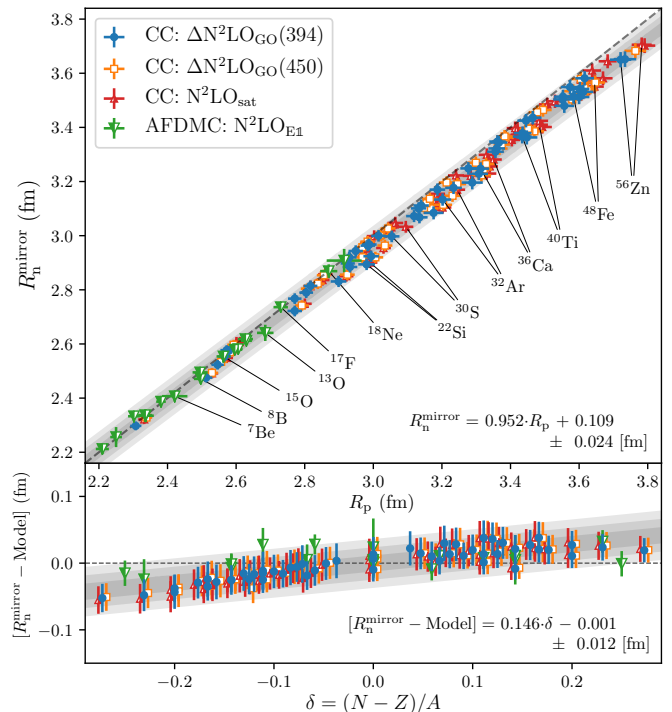


Figure 3. Top panel: Point-neutron radius plotted against the point-proton radius of the corresponding mirror nucleus. The data markers are the same as those in Fig. 1. The linear regression is printed in the bottom right with  $1\sigma$  uncertainty, and the  $1\sigma$ ,  $2\sigma$ , and  $3\sigma$  confidence levels are shown as overlapping gray bands. Selected neutron-deficient nuclei are labeled, and the  $R_{\text{p}} = R_{\text{n}}^{\text{mirror}}$  line is shown as a visual reference. Bottom panel: Residuals between data and linear model of the top panel, plotted against the isospin asymmetry.

necting mirror radii with isospin-symmetry dependence,  $R_{\text{n}}^{\text{mirror}} = 0.952 \cdot R_{\text{p}} + 0.146 \cdot \delta + 0.108 \pm 0.011$  fm. This analysis is useful because neutron distributions are very difficult to measure experimentally, so the proton radius, much easier to measure, can be used as a surrogate.

The near-equivalence between  $R_{\text{n}}^{\text{mirror}}$  and  $R_{\text{p}}$ , shown in Fig. 3, indicates a direct relation between the neutron skin and the mirror-difference charge radii,  $\Delta R_{\text{ch}}^{\text{mirror}} = [R_{\text{ch}}(^A\text{Y}_Z) - R_{\text{ch}}(^A\text{X}_N)]$ . Recently, calculations based on energy density functional theories [14, 85, 87] have shown a correlation between  $\Delta R_{\text{ch}}^{\text{mirror}}$  and the symmetry energy slope at saturation,  $L$ . This finding has enabled recent high-precision measurements of charge radii of the neutron-deficient isotopes  $^{36}\text{Ca}$  [19] and  $^{54}\text{Ni}$  [85] to constrain  $L$  in the range  $20 \leq L \leq 70$  MeV. We note that this range is consistent with the range for  $L$  from the different interactions used in this work,  $40.8 \leq L \leq 65.2$  MeV. To compare with data and the conclusions drawn from the mean-field calculations of [85], we compute the mirror-difference charge radii for selected nuclei shown in Fig. 4. The charge radius is computed using the formula  $R_{\text{ch}}^2 = R_{\text{p}}^2 + \langle r_{\text{p}}^2 \rangle + \frac{N}{Z} \langle r_{\text{n}}^2 \rangle + \langle r_{\text{DF}}^2 \rangle + \langle r_{\text{SO}}^2 \rangle$  where

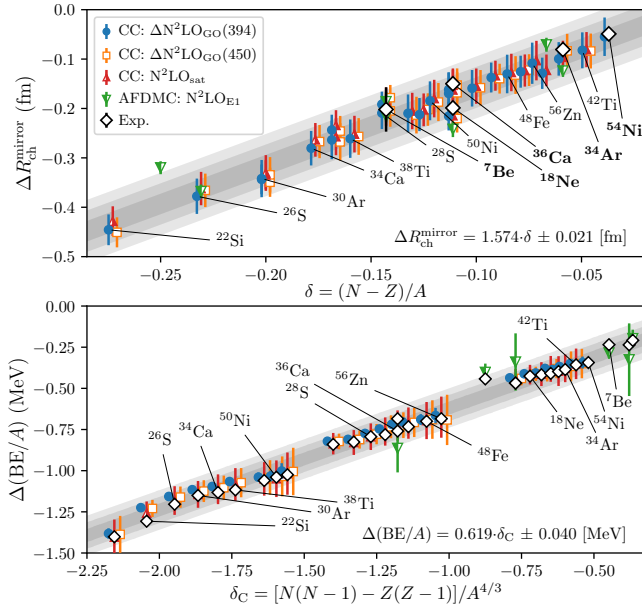


Figure 4. Top panel: Mirror-difference charge radii plotted against the isospin asymmetry compared with experiment. The data markers are the same as those in Fig. 1. The linear regression of our data is printed in the bottom left with  $1\sigma$  uncertainty, and the  $1\sigma$ ,  $2\sigma$ , and  $3\sigma$  confidence levels are shown as overlapping gray bands. Selected neutron-deficient nuclei are labeled. Experimental data are shown as open white diamonds, taken from Ref. [25] except for those of  $^{36}\text{Ca}$  [19] and  $^{54}\text{Ni}$  [85]. Bottom panel: Mirror-difference binding energy per nucleon  $\Delta(\text{BE}/A)$  as a function of the Coulomb asymmetry. Experimental data are taken from Ref. [86].

the spin-orbit correction,  $\langle r_{\text{SO}}^2 \rangle$ , is calculated with the CC method [13], and  $\langle r_{\text{p}}^2 \rangle = 0.709 \text{ fm}^2$ ,  $\langle r_{\text{n}}^2 \rangle = -0.106 \text{ fm}^2$ , and  $\langle r_{\text{DF}}^2 \rangle = 3/(4m^2) = 0.033 \text{ fm}^2$  are the charge radius squared of the proton [88, 89], the neutron [90], and the Darwin-Foldy term, respectively, with  $m$  being the nucleon mass. Our results agree well with the sparse data, most of which were taken from Ref. [25] except for those of  $^{36}\text{Ca}$  [19] and  $^{54}\text{Ni}$  [85]. Because  $\Delta R_{\text{ch}}^{\text{mirror}}$  is an analogue of the neutron skin, it also has a linear relation to the isospin asymmetry. Also shown in Fig. 4 is the comparison of our results with data from Ref. [86] of mirror-difference binding energies per nucleon ( $\Delta(\text{BE}/A) = [\text{BE}(\frac{A}{2}X_N) - \text{BE}(\frac{A}{2}Y_Z)]/A$ ). This quantity exhibits a linear relationship with the Coulomb asymmetry,  $\delta_{\text{C}} = [N(N-1) - Z(Z-1)]/A^{4/3}$ , which stems from the only mirror-asymmetric term in the liquid-drop model.

Finally, we also study the extent of the isospin-symmetry-breaking terms in the nuclear interaction by computing ground-state energies and radii of select mirror nuclei using CC theory with and without the Coulomb term. We show these results for  $A = 42 - 48$  using  $\Delta\text{N}^2\text{LO}_{\text{GO}}(394)$  in Table I, as the neutron skin thickness, the mirror-difference charge radius, and the mirror-difference binding energy per nucleon. Like their corre-

Table I. Neutron skin thickness ( $\Delta R_{\text{np}}$ ), mirror-difference charge radius ( $\Delta R_{\text{ch}}^{\text{mirror}}$ ), and mirror-difference binding energy per nucleon ( $\Delta(\text{BE}/A)$ ) of select nuclei using  $\Delta\text{N}^2\text{LO}_{\text{GO}}(394)$  with and without the Coulomb term.

$\Delta R_{\text{np}}$ (fm)	Full	w/o Coulomb
$^{42}\text{Ca}$	0.019(35)	0.060(34)
$^{46}\text{Ca}$	0.113(35)	0.151(35)
$^{48}\text{Cr}$	-0.048(38)	-0.002(36)
$^{48}\text{Ti}$	0.049(37)	0.090(36)
$^{48}\text{Ca}$	0.150(36)	0.186(35)
$\Delta R_{\text{ch}}^{\text{mirror}}$ (fm)		
$^{42}\text{Ca}$	0.075(36)	0.082(33)
$^{46}\text{Ca}$	0.191(38)	0.209(35)
$^{48}\text{Ti}$	0.119(38)	0.128(36)
$^{48}\text{Ca}$	0.238(38)	0.261(35)
$\Delta(\text{BE}/A)$ (MeV)		
$^{42}\text{Ca}$	0.349(04)	0.0038(5)
$^{46}\text{Ca}$	1.039(11)	0.0113(1)
$^{48}\text{Ti}$	0.689(75)	0.0075(1)
$^{48}\text{Ca}$	1.381(15)	0.0150(2)

sponding quantities calculated with the Coulomb term,  $\Delta R_{\text{np}}$  and  $\Delta R_{\text{ch}}^{\text{mirror}}$  both exhibit a linear relationship with the isospin asymmetry. However, unlike the relation shown in Fig. 4,  $\Delta(\text{BE}/A)$  also exhibits a linear relationship with the isospin asymmetry without the Coulomb term. By removing the Coulomb term to approximate isospin symmetry, the near equivalence between  $\Delta R_{\text{np}}$  and  $\Delta R_{\text{ch}}^{\text{mirror}}$  shows the validity of this approximation. Additionally, the  $\Delta(\text{BE}/A)$  results without the Coulomb interaction entirely reflect the effects of the isospin-symmetry-breaking terms in the chiral interaction, accounting for only  $\sim 1\%$  of  $\Delta(\text{BE}/A)$ . These results can be used to constrain the charge-symmetry-breaking term in Skyrme density functional theory according to Ref. [91].

*Conclusions.*— We performed CC and AFDMC calculations of neutron skins of a wide range of light- and medium-mass nuclei using different interactions from chiral EFT, and found a robust linear relationship with the isospin asymmetry. When extrapolated to heavy nuclei, this relationship is consistent with the available data. Additionally, we found a linear relationship between the neutron and proton radii of mirror nuclei pairs which can be used to estimate neutron radii of rare isotopes not yet accessible by experiment. Our calculations are in good agreement with available data for the difference in charge radii and binding energies of mirror nuclei. Finally, we estimated the contributions from charge-symmetry-breaking terms in the nuclear interaction which can be useful for constraining those terms in Skyrme density functionals.

We would like to thank J. Carlson, I. Tews, and R. F. Garcia Ruiz for helpful discussions. The work of S. G., S. N., and D. L. was supported by the DOE NUCLEI SciDAC Program, and by the DOE Early Career Research Program. The work of S. G. was also supported by U.S. Department of Energy, Office of Science, Office of Nuclear Physics, under Contract No. DE-AC52-06NA25396. G. H. was supported by the Office of Nuclear Physics, U.S. Department of Energy, under grants DE-SC0018223 (NUCLEI SciDAC-4 collaboration) and by the Field Work Proposal ERKBP72 at Oak Ridge National Laboratory (ORNL). Computer time was provided by the Innovative and Novel Computational Impact on Theory and Experiment (INCITE) program. This research used resources of the Oak Ridge Leadership Computing Facility located at ORNL, which is supported by the Office of Science of the Department of Energy under Contract No. DE-AC05-00OR22725. This research also used resources provided by the Los Alamos National Laboratory Institutional Computing Program, which is supported by the U.S. Department of Energy National Nuclear Security Administration under Contract No. 89233218CNA000001.

- 
- [1] B. Alex Brown, Neutron radii in nuclei and the neutron equation of state, *Phys. Rev. Lett.* **85**, 5296 (2000).
- [2] C. J. Horowitz and J. Piekarewicz, Neutron star structure and the neutron radius of  $^{208}\text{Pb}$ , *Phys. Rev. Lett.* **86**, 5647 (2001).
- [3] C. J. Horowitz and J. Piekarewicz, Neutron radii of  $^{208}\text{Pb}$  and neutron stars, *Phys. Rev. C* **64**, 062802 (2001).
- [4] S. Gandolfi, J. Carlson, and S. Reddy, Maximum mass and radius of neutron stars, and the nuclear symmetry energy, *Phys. Rev. C* **85**, 032801 (2012).
- [5] B. P. Abbott, R. Abbott, T. D. Abbott, F. Acernese, K. Ackley, C. Adams, T. Adams, P. Addesso, R. X. Adhikari, V. B. Adya, C. Affeldt, M. Afrough, B. Agarwal, M. Agathos, K. Agatsuma, *et al.* (LIGO Scientific Collaboration and Virgo Collaboration), GW170817: Observation of gravitational waves from a binary neutron star inspiral, *Phys. Rev. Lett.* **119**, 161101 (2017).
- [6] B. P. Abbott, R. Abbott, T. D. Abbott, F. Acernese, K. Ackley, C. Adams, T. Adams, P. Addesso, R. X. Adhikari, V. B. Adya, C. Affeldt, M. Afrough, B. Agarwal, M. Agathos, K. Agatsuma, *et al.*, Multi-messenger observations of a binary neutron star merger, *ApJ* **848**, L12 (2017).
- [7] M. Al-Mamun, A. W. Steiner, J. Nättilä, J. Lange, R. O’Shaughnessy, I. Tews, S. Gandolfi, C. Heinke, and S. Han, Combining electromagnetic and gravitational-wave constraints on neutron-star masses and radii, *Phys. Rev. Lett.* **126**, 061101 (2021).
- [8] S. Abrahamyan, Z. Ahmed, H. Albatineh, K. Aniol, D. S. Armstrong, W. Armstrong, T. Averett, B. Babineau, A. Barbieri, V. Bellini, R. Beminiwaththa, J. Benesch, F. Benmokhtar, T. Bielarski, W. Boeglin, *et al.* (PREX Collaboration), Measurement of the neutron radius of  $^{208}\text{Pb}$  through parity violation in electron scattering, *Phys. Rev. Lett.* **108**, 112502 (2012).
- [9] D. Adhikari, H. Albatineh, D. Androic, K. Aniol, D. S. Armstrong, T. Averett, C. Ayerbe Gayoso, S. Barcus, V. Bellini, R. S. Beminiwaththa, J. F. Benesch, H. Bhatt, D. Bhatta Pathak, D. Bhetuwal, B. Blaikie, *et al.* (PREX Collaboration), Accurate determination of the neutron skin thickness of  $^{208}\text{Pb}$  through parity-violation in electron scattering, *Phys. Rev. Lett.* **126**, 172502 (2021).
- [10] Mammei, J. and McNulty, D. and Michaels, R. and Paschke, K. and Riordan, S. and Souder, P. A., CREX: Parity-violating measurement of the weak charge distribution of  $^{48}\text{Ca}$  to 0.02 fm accuracy, [https://hallaweb.jlab.org/parity/prex/c-rex2013\\_v7.pdf](https://hallaweb.jlab.org/parity/prex/c-rex2013_v7.pdf) (2013).
- [11] C. J. Horowitz, K. S. Kumar, and R. Michaels, Electroweak measurements of neutron densities in CREX and PREX at JLab, USA, *EPJA* **50**, 48 (2014).
- [12] M. B. Tsang, J. R. Stone, F. Camera, P. Danielewicz, S. Gandolfi, K. Hebeler, C. J. Horowitz, J. Lee, W. G. Lynch, Z. Kohley, R. Lemmon, P. Möller, T. Murakami, S. Riordan, X. Roca-Maza, F. Sammarruca, A. W. Steiner, I. Vidaña, and S. J. Yennello, Constraints on the symmetry energy and neutron skins from experiments and theory, *Phys. Rev. C* **86**, 015803 (2012).
- [13] G. Hagen, A. Ekström, C. Forssén, G. R. Jansen, W. Nazarewicz, T. Papenbrock, K. A. Wendt, S. Bacca, N. Barnea, B. Carlsson, C. Drischler, K. Hebeler, M. Hjorth-Jensen, M. Miorelli, G. Orlandini, A. Schwenk, and J. Simonis, Neutron and weak-charge distributions of the  $^{48}\text{Ca}$  nucleus, *Nat. Phys.* **12**, 186 (2016).
- [14] B. A. Brown, Mirror charge radii and the neutron equation of state, *Phys. Rev. Lett.* **119**, 122502 (2017).
- [15] F. J. Fattoyev, J. Piekarewicz, and C. J. Horowitz, Neutron skins and neutron stars in the multimessenger era, *Phys. Rev. Lett.* **120**, 172702 (2018).
- [16] C. A. Bertulani and J. Valencia, Neutron skins as laboratory constraints on properties of neutron stars and on what we can learn from heavy ion fragmentation reactions, *Phys. Rev. C* **100**, 015802 (2019).
- [17] Á. Koszorús, X. F. Yang, W. G. Jiang, S. J. Novario, S. W. Bai, J. Billowes, C. L. Binnersley, M. L. Bissell, T. E. Cocolios, B. S. Cooper, R. P. de Groote, A. Ekström, K. T. Flanagan, C. Forssén, S. Franchoo, R. F. G. Ruiz, F. P. Gustafsson, G. Hagen, G. R. Jansen, A. Kanellakopoulos, M. Kortelainen, W. Nazarewicz, G. Neyens, T. Papenbrock, P.-G. Reinhard, C. M. Ricketts, B. K. Sahoo, A. R. Vernon, and S. G. Wilkins, Charge radii of exotic potassium isotopes challenge nuclear theory and the magic character of  $N = 32$ , *Nat. Phys.* **17**, 439 (2021).
- [18] R. F. Garcia Ruiz, M. L. Bissell, K. Blaum, A. Ekström, N. Frömmgen, G. Hagen, M. Hammen, K. Hebeler, J. D. Holt, G. R. Jansen, M. Kowalska, K. Kreim, W. Nazarewicz, R. Neugart, G. Neyens, W. Nörtershäuser, T. Papenbrock, J. Papuga, A. Schwenk, J. Simonis, K. A. Wendt, and D. T. Yordanov, Unexpectedly large charge radii of neutron-rich calcium isotopes, *Nat. Phys.* **12**, 594 (2016).
- [19] A. J. Miller, K. Minamisono, A. Klose, D. Garand, C. Kujawa, J. D. Lantis, Y. Liu, B. Maaß, P. F. Mantica, W. Nazarewicz, W. Nörtershäuser, S. V. Pineda, P. G. Reinhard, D. M. Rossi, F. Sommer, C. Sumithrarachchi, A. Teigelhöfer, and J. Watkins, Proton superfluidity and charge radii in proton-rich calcium isotopes, *Nat. Phys.*

- 15**, 432 (2019).
- [20] S. Malbrunot-Ettenauer and et.al., to be published (2021).
- [21] M. L. Bissell, T. Carette, K. T. Flanagan, P. Vingerhoets, J. Billowes, K. Blaum, B. Cheal, S. Fritzsche, M. Godefroid, M. Kowalska, J. Krämer, R. Neugart, G. Neyens, W. Nörtershäuser, and D. T. Jordanov, Cu charge radii reveal a weak sub-shell effect at  $N = 40$ , *Phys. Rev. C* **93**, 064318 (2016).
- [22] R. P. de Groote, J. Billowes, C. L. Binnersley, M. L. Bissell, T. E. Cocolios, T. Day Goodacre, G. J. Farooq-Smith, D. V. Fedorov, K. T. Flanagan, S. Franchoo, R. F. Garcia Ruiz, W. Gins, J. D. Holt, Á. Koszorús, K. M. Lynch, T. Miyagi, W. Nazarewicz, G. Neyens, P. G. Reinhard, S. Rothe, H. H. Stroke, A. R. Vernon, K. D. A. Wendt, S. G. Wilkins, Z. Y. Xu, and X. F. Yang, Measurement and microscopic description of odd-even staggering of charge radii of exotic copper isotopes, *Nat. Phys.* **16**, 620 (2020).
- [23] M. Reponen, R. P. de Groote, L. Al Ayoubi, O. Beliuskina, M. L. Bissell, P. Campbell, L. Cañete, B. Cheal, K. Chrysalidis, C. Delafosse, A. de Roubin, C. S. Devlin, T. Eronen, R. F. Garcia Ruiz, S. Geldhof, W. Gins, M. Hukkanen, P. Ingram, A. Kankainen, M. Kortelainen, Á. Koszorús, S. Kujanpää, R. Mathieson, D. A. Nesterenko, I. Pohjalainen, M. Vilén, A. Zadornaya, and I. D. Moore, Evidence of a sudden increase in the nuclear size of proton-rich silver-96, *Nat. Comm.* **12**, 4596 (2021).
- [24] C. De Jager, H. De Vries, and C. De Vries, Nuclear charge- and magnetization-density-distribution parameters from elastic electron scattering, *Atomic Data and Nuclear Data Tables* **14**, 479 (1974), nuclear Charge and Moment Distributions.
- [25] I. Angeli and K. Marinova, Table of experimental nuclear ground state charge radii: An update, *Atomic Data and Nuclear Data Tables* **99**, 69 (2013).
- [26] J. Piekarewicz and S. Weppner, Insensitivity of the elastic proton-nucleus reaction to the neutron radius of  $^{208}\text{Pb}$ , *Nucl. Phys. A* **778**, 10 (2006).
- [27] T. Donnelly, J. Dubach, and I. Sick, Isospin dependences in parity-violating electron scattering, *Nucl. Phys. A* **503**, 589 (1989).
- [28] F. Coester, Bound states of a many-particle system, *Nucl. Phys.* **7**, 421 (1958).
- [29] F. Coester and H. Kümmel, Short-range correlations in nuclear wave functions, *Nucl. Phys.* **17**, 477 (1960).
- [30] J. Čížek, On the correlation problem in atomic and molecular systems. calculation of wavefunction components in Ursell-type expansion using quantum-field theoretical methods, *J. Chem. Phys.* **45**, 4256 (1966).
- [31] J. Čížek, On the use of the cluster expansion and the technique of diagrams in calculations of correlation effects in atoms and molecules, in *Advances in Chemical Physics* (John Wiley & Sons, Inc., 2007) pp. 35–89.
- [32] H. Kümmel, K. H. Lührmann, and J. G. Zabolitzky, Many-fermion theory in expS- (or coupled cluster) form, *Phys. Rep.* **36**, 1 (1978).
- [33] R. J. Bartlett and M. Musiał, Coupled-cluster theory in quantum chemistry, *Rev. Mod. Phys.* **79**, 291 (2007).
- [34] G. Hagen, T. Papenbrock, M. Hjorth-Jensen, and D. J. Dean, Coupled-cluster computations of atomic nuclei, *Rep. Prog. Phys.* **77**, 096302 (2014).
- [35] K. E. Schmidt and S. Fantoni, A quantum Monte Carlo method for nucleon systems, *Phys. Lett. B* **446**, 99 (1999).
- [36] J. Carlson, S. Gandolfi, F. Pederiva, S. C. Pieper, R. Schiavilla, K. E. Schmidt, and R. B. Wiringa, Quantum monte carlo methods for nuclear physics, *Rev. Mod. Phys.* **87**, 1067 (2015).
- [37] D. Lonardonì, S. Gandolfi, J. E. Lynn, C. Petrie, J. Carlson, K. E. Schmidt, and A. Schwenk, Auxiliary field diffusion Monte Carlo calculations of light and medium-mass nuclei with local chiral interactions, *Phys. Rev. C* **97**, 044318 (2018).
- [38] E. Epelbaum, H.-W. Hammer, and U.-G. Meißner, Modern theory of nuclear forces, *Rev. Mod. Phys.* **81**, 1773 (2009).
- [39] R. Machleidt and D. Entem, Chiral effective field theory and nuclear forces, *Phys. Rep.* **503**, 1 (2011).
- [40] K. Hebeler, S. K. Bogner, R. J. Furnstahl, A. Nogga, and A. Schwenk, Improved nuclear matter calculations from chiral low-momentum interactions, *Phys. Rev. C* **83**, 031301 (2011).
- [41] A. Ekström, G. Baardsen, C. Forssén, G. Hagen, M. Hjorth-Jensen, G. R. Jansen, R. Machleidt, W. Nazarewicz, T. Papenbrock, J. Sarich, and S. M. Wild, Optimized chiral nucleon-nucleon interaction at next-to-next-to-leading order, *Phys. Rev. Lett.* **110**, 192502 (2013).
- [42] D. R. Entem, N. Kaiser, R. Machleidt, and Y. Nosyk, Peripheral nucleon-nucleon scattering at fifth order of chiral perturbation theory, *Phys. Rev. C* **91**, 014002 (2015).
- [43] E. Epelbaum, H. Krebs, and U.-G. Meißner, Precision nucleon-nucleon potential at fifth order in the chiral expansion, *Phys. Rev. Lett.* **115**, 122301 (2015).
- [44] T. Hüther, K. Vobig, K. Hebeler, R. Machleidt, and R. Roth, Family of chiral two- plus three-nucleon interactions for accurate nuclear structure studies, *Phys. Lett. B* **808**, 135651 (2020).
- [45] V. Somà, P. Navrátil, F. Raimondi, C. Barbieri, and T. Duguet, Novel chiral Hamiltonian and observables in light and medium-mass nuclei, *Phys. Rev. C* **101**, 014318 (2020).
- [46] A. Ekström, B. D. Carlsson, K. A. Wendt, C. Forssén, M. H. Jensen, R. Machleidt, and S. M. Wild, Statistical uncertainties of a chiral interaction at next-to-next-to leading order, *J. Phys., G: Nucl. Part. Phys.* **42**, 034003 (2015).
- [47] C. G. Payne, S. Bacca, G. Hagen, W. G. Jiang, and T. Papenbrock, Coherent elastic neutrino-nucleus scattering on  $^{40}\text{Ar}$  from first principles, *Phys. Rev. C* **100**, 061304 (2019).
- [48] S. Bagchi, R. Kanungo, Y. K. Tanaka, H. Geissel, P. Doornenbal, W. Horiuchi, G. Hagen, T. Suzuki, N. Tsunoda, D. S. Ahn, H. Baba, K. Behr, F. Browne, S. Chen, M. L. Cortés, A. Estradé, N. Fukuda, M. Holl, K. Itahashi, N. Iwasa, G. R. Jansen, W. G. Jiang, S. Kaur, A. O. Macchiavelli, S. Y. Matsumoto, S. Momiyama, I. Murray, T. Nakamura, S. J. Novario, H. J. Ong, T. Otsuka, T. Papenbrock, S. Paschalis, A. Prochazka, C. Scheidenberger, P. Schrock, Y. Shimizu, D. Steppenbeck, H. Sakurai, D. Suzuki, H. Suzuki, M. Takechi, H. Takeda, S. Takeuchi, R. Taniuchi, K. Wimmer, and K. Yoshida, Two-neutron halo is unveiled in  $^{29}\text{F}$ , *Phys. Rev. Lett.* **124**, 222504 (2020).
- [49] W. G. Jiang, A. Ekström, C. Forssén, G. Hagen, G. R. Jansen, and T. Papenbrock, Accurate bulk properties of nuclei from  $A = 2$  to  $\infty$  from potentials with  $\Delta$  isobars,

- Phys. Rev. C* **102**, 054301 (2020).
- [50] A. Tichai, J. Müller, K. Vobig, and R. Roth, Natural orbitals for ab initio no-core shell model calculations, *Phys. Rev. C* **99**, 034321 (2019).
- [51] S. J. Novario, G. Hagen, G. R. Jansen, and T. Papenbrock, Charge radii of exotic neon and magnesium isotopes, *Phys. Rev. C* **102**, 051303 (2020).
- [52] G. Hagen, T. Papenbrock, D. J. Dean, A. Schwenk, A. Nogga, M. Włoch, and P. Piecuch, Coupled-cluster theory for three-body Hamiltonians, *Phys. Rev. C* **76**, 034302 (2007).
- [53] R. Roth, S. Binder, K. Vobig, A. Calci, J. Langhammer, and P. Navrátil, Medium-mass nuclei with normal-ordered chiral  $NN+3N$  interactions, *Phys. Rev. Lett.* **109**, 052501 (2012).
- [54] A. Gezerlis, I. Tews, E. Epelbaum, S. Gandolfi, K. Hebeler, A. Nogga, and A. Schwenk, Quantum Monte Carlo calculations with chiral effective field theory interactions, *Phys. Rev. Lett.* **111**, 032501 (2013).
- [55] A. Gezerlis, I. Tews, E. Epelbaum, M. Freunek, S. Gandolfi, K. Hebeler, A. Nogga, and A. Schwenk, Local chiral effective field theory interactions and quantum Monte Carlo applications, *Phys. Rev. C* **90**, 054323 (2014).
- [56] J. E. Lynn, I. Tews, J. Carlson, S. Gandolfi, A. Gezerlis, K. E. Schmidt, and A. Schwenk, Chiral three-nucleon interactions in light nuclei, neutron- $\alpha$  scattering, and neutron matter, *Phys. Rev. Lett.* **116**, 062501 (2016).
- [57] J. E. Lynn, J. Carlson, E. Epelbaum, S. Gandolfi, A. Gezerlis, and A. Schwenk, Quantum Monte Carlo calculations of light nuclei using chiral potentials, *Phys. Rev. Lett.* **113**, 192501 (2014).
- [58] J. E. Lynn, I. Tews, J. Carlson, S. Gandolfi, A. Gezerlis, K. E. Schmidt, and A. Schwenk, Quantum Monte Carlo calculations of light nuclei with local chiral two- and three-nucleon interactions, *Phys. Rev. C* **96**, 054007 (2017).
- [59] D. Lonardoni, J. Carlson, S. Gandolfi, J. E. Lynn, K. E. Schmidt, A. Schwenk, and X. B. Wang, Properties of nuclei up to  $A = 16$  using local chiral interactions, *Phys. Rev. Lett.* **120**, 122502 (2018).
- [60] D. Lonardoni, S. Gandolfi, X. B. Wang, and J. Carlson, Single- and two-nucleon momentum distributions for local chiral interactions, *Phys. Rev. C* **98**, 014322 (2018).
- [61] J. E. Lynn, D. Lonardoni, J. Carlson, J.-W. Chen, W. Detmold, S. Gandolfi, and A. Schwenk, Ab initio short-range-correlation scaling factors from light to medium-mass nuclei, *J. Phys. G: Nucl. Part. Phys.* **47**, 045109 (2020).
- [62] S. H. Lim, J. Carlson, C. Loizides, D. Lonardoni, J. E. Lynn, J. L. Nagle, J. D. Orjuela Koop, and J. Ouellette, Exploring new small system geometries in heavy ion collisions, *Phys. Rev. C* **99**, 044904 (2019).
- [63] R. Cruz-Torres, S. Li, F. Hauenstein, A. Schmidt, D. Nguyen, D. Abrams, H. Albatineh, S. Alsalmi, D. Androic, K. Aniol, W. Armstrong, J. Arrington, H. Atac, T. Averett, C. Ayerbe Gayoso, *et al.*, Comparing proton momentum distributions in  $A = 2$  and 3 nuclei via  $^2\text{H}$ ,  $^3\text{H}$  and  $^3\text{He}$  ( $e, e'p$ ) measurements, *Phys. Lett. B* **797**, 134890 (2019).
- [64] R. Cruz-Torres, D. Lonardoni, R. Weiss, M. Pirulli, N. Barnea, D. W. Higinbotham, E. Piasetzky, A. Schmidt, L. B. Weinstein, R. B. Wiringa, and O. Hen, Many-body factorization and position-momentum equivalence of nuclear short-range correlations, *Nat. Phys.* **17**, 306 (2021).
- [65] P. W. Zhao and S. Gandolfi, Radii of neutron drops probed via the neutron skin thickness of nuclei, *Phys. Rev. C* **94**, 041302 (2016).
- [66] P. Klos, J. E. Lynn, I. Tews, S. Gandolfi, A. Gezerlis, H.-W. Hammer, M. Hoferichter, and A. Schwenk, Quantum Monte Carlo calculations of two neutrons in finite volume, *Phys. Rev. C* **94**, 054005 (2016).
- [67] S. Gandolfi, H.-W. Hammer, P. Klos, J. E. Lynn, and A. Schwenk, Is a trineutron resonance lower in energy than a tetra-neutron resonance?, *Phys. Rev. Lett.* **118**, 232501 (2017).
- [68] I. Tews, S. Gandolfi, A. Gezerlis, and A. Schwenk, Quantum Monte Carlo calculations of neutron matter with chiral three-body forces, *Phys. Rev. C* **93**, 024305 (2016).
- [69] M. Buraczynski and A. Gezerlis, Static response of neutron matter, *Phys. Rev. Lett.* **116**, 152501 (2016).
- [70] M. Buraczynski and A. Gezerlis, Ab initio and phenomenological studies of the static response of neutron matter, *Phys. Rev. C* **95**, 044309 (2017).
- [71] L. Riz, S. Gandolfi, and F. Pederiva, Spin response and neutrino mean free path in neutron matter, *J. Phys. G: Nucl. Part. Phys.* **47**, 045106 (2020).
- [72] I. Tews, J. Carlson, S. Gandolfi, and S. Reddy, Constraining the speed of sound inside neutron stars with chiral effective field theory interactions and observations, *ApJ* **860**, 149 (2018).
- [73] I. Tews, J. Margueron, and S. Reddy, Critical examination of constraints on the equation of state of dense matter obtained from GW170817, *Phys. Rev. C* **98**, 045804 (2018).
- [74] S. Gandolfi, J. Carlson, A. Roggero, J. E. Lynn, and S. Reddy, Small bits of cold dense matter, *Phys. Lett. B* **785**, 232 (2018).
- [75] I. Tews, J. Margueron, and S. Reddy, Confronting gravitational-wave observations with modern nuclear physics constraints, *EPJA* **55**, 97 (2019).
- [76] D. Lonardoni, I. Tews, S. Gandolfi, and J. Carlson, Nuclear and neutron-star matter from local chiral interactions, *Phys. Rev. Research* **2**, 022033 (2020).
- [77] L. Riz, F. Pederiva, D. Lonardoni, and S. Gandolfi, Spin susceptibility in neutron matter from quantum Monte Carlo calculations, *Particles* **3**, 706 (2020).
- [78] C. J. Pethick and D. G. Ravenhall, The dependence of neutron skin thickness and surface tension on neutron excess, *Nucl. Phys. A* **606**, 173 (1996).
- [79] S. Kaufmann, J. Simonis, S. Bacca, J. Billowes, M. L. Bissell, K. Blaum, B. Cheal, R. F. G. Ruiz, W. Gins, C. Gorges, G. Hagen, H. Heylen, A. Kanellakopoulos, S. Malbrunot-Ettenauer, M. Miorelli, R. Neugart, G. Neyens, W. Nörtershäuser, R. Sánchez, S. Sailer, A. Schwenk, T. Ratajczyk, L. V. Rodríguez, L. Wehner, C. Wraith, L. Xie, Z. Y. Xu, X. F. Yang, and D. T. Yordanov, Charge radius of the short-lived  $^{68}\text{Ni}$  and correlation with the dipole polarizability, *Phys. Rev. Lett.* **124**, 132502 (2020).
- [80] M. Miorelli, S. Bacca, G. Hagen, and T. Papenbrock, Computing the dipole polarizability of  $^{48}\text{Ca}$  with increased precision, *Phys. Rev. C* **98**, 014324 (2018).
- [81] G. Hagen, S. J. Novario, Z. H. Sun, T. Papenbrock, G. R. Jansen, J. G. Lietz, T. Duguet, and A. Tichai, to be published (2021).
- [82] A. Trzcńska, J. Jastrzębski, P. Lubiński, F. J. Hartmann, R. Schmidt, T. von Egidy, and B. Klos, Neutron Density

- Distributions Deduced from Antiprotonic Atoms, *Phys. Rev. Lett.* **87**, 082501 (2001).
- [83] J. Jastrzębski, A. Trzczińska, P. Lubiński, B. Kłos, F. J. Hartmann, T. von Egidy, and S. Wycech, Neutron density distributions from antiprotonic atoms compared with hadron scattering data, *Int. J. Mod. Phys. E* **13**, 343 (2004).
- [84] B. T. Reed, F. J. Fattoyev, C. J. Horowitz, and J. Piekarewicz, Implications of PREX-2 on the equation of state of neutron-rich matter, *Phys. Rev. Lett.* **126**, 172503 (2021).
- [85] S. V. Pineda, K. König, D. M. Rossi, B. A. Brown, A. Incorvati, J. Lantis, K. Minamisono, W. Nörtershäuser, J. Piekarewicz, R. Powel, and F. Sommer, Charge radius of neutron-deficient  $^{54}\text{Ni}$  and symmetry energy constraints using the difference in mirror pair charge radii, *Phys. Rev. Lett.* **127**, 182503 (2021).
- [86] M. Wang, G. Audi, F. G. Kondev, W. Huang, S. Naimi, and X. Xu, The AME2016 atomic mass evaluation (II). tables, graphs and references, *Chinese Physics C* **41**, 030003 (2017).
- [87] J. Yang and J. Piekarewicz, Difference in proton radii of mirror nuclei as a possible surrogate for the neutron skin, *Phys. Rev. C* **97**, 014314 (2018).
- [88] R. Pohl, A. Antognini, F. Nez, F. D. Amaro, F. Biraben, J. M. Cardoso, D. S. Covita, A. Dax, S. Dhawan, L. M. Fernandes, A. Giesen, T. Graf, T. W. Hänsch, P. Indelicato, L. Julien, *et al.*, The size of the proton, *Nature* **466**, 213 (2010).
- [89] W. Xiong, A. Gasparian, H. Gao, D. Dutta, M. Khandaker, N. Liyanage, E. Pasyuk, C. Peng, X. Bai, L. Ye, K. Gnanvo, C. Gu, M. Levillain, X. Yan, D. W. Higinbotham, *et al.*, A small proton charge radius from an electron–proton scattering experiment, *Nature* **575**, 147 (2019).
- [90] A. A. Filin, V. Baru, E. Epelbaum, H. Krebs, D. Möller, and P. Reinert, Extraction of the neutron charge radius from a precision calculation of the deuteron structure radius, *Phys. Rev. Lett.* **124**, 082501 (2020).
- [91] T. Naito, G. Coló, H. Liang, X. Roca-Maza, and H. Sagawa, Toward ab initio determination of charge symmetry breaking strength of Skyrme functionals (2021), [arXiv:2107.14436 \[nucl-th\]](https://arxiv.org/abs/2107.14436).